UDK 661.66/.68:537.874.31
Original scientific article/Izvirni znanstveni članek

ISSN 1580-2949
MTAEC9, 57(2)169(2023)

CORRELATION BETWEEN ELECTRICAL AND OPTICAL PROPERTIES OF DOPED SILICON NANOCRYSTALS

KORELACIJA MED ELEKTRIČNIMI IN OPTIČNIMI LASTNOSTMI DOPIRANIH SILICIJEVIH NANOKRISTALOV

Hakim Haoues[1,2], Hachemi Bouridah[1,2], Amir Ferrah[1], Nidal Beltas[1], Mahmoud Riad Beghoul[1,2], Riad Remmouche[1,2]

[1]Department of Electronics, University of Jijel, Ouled Aissa 18000, Jijel, Algeria
[2]Laboratory of Materials Studies, University of Jijel, Ouled Aissa 18000, Jijel, Algeria

Prejem rokopisa – received: 2022-12-21; sprejem za objavo – accepted for publication: 2023-02-15

doi:10.17222/mit.2022.720

We propose through this work a correlation method leading to a determination of a semi-empirical relationship between optical and electrical properties in terms of refractive index and dark conductivity of doped silicon nanocrystals based on experimental data published in literature. First, an analytical model relating the conductivity and bandgap of doped silicon nanocrystals was derived. Using an empirical expression relating the refractive index to the bandgap energy, we correlated the electrical and optical parameters of N-type nanocrystalline silicon with a semi-empirical expression. The semi-empirical relationship was found to account correctly for the experimental results and yield a reasonably good agreement in an interval of the bandgap energy variation of N-type silicon nanocrystal films. The values of the fitting parameters were calculated for the N-type silicon nanocrystal films having their bandgap energy between 1. 7 eV and 2.2 eV.

Keywords: silicon nanocystals, doping, dark conductivity, refractive index

V članku je predstavljeno delo v katerem so s pomočjo korelacijske metode določili polempirično povezavo med optičnimi in električnimi lastnostmi dopiranih silicijevih nanokristalov. Dejansko podana korelacija predstavlja zvezo med lomnim količnikom in temno prevodnostjo, ki so jo dobili s pomočjo eksperimentalnih podatkov najdenih v literaturi. Na začetku so postavili analitični model, ki se nanaša na prevodnost in energijski prevodni pas elektronov dopiranih nanokristalov. S postavitvijo empiričnega izraza, ki povezuje lomni količnik in energijo v prepovedanem energijskem pasu so s pomočjo polempiričnega izraza povezali električne in optične parametre N-tipa nanokristaliničnega silicija. Ugotovili so, da se polempirična zveza točno ujema z eksperimentalnimi rezultati in dokaj dobro ujema v intervalu v katerem se nahaja energija prepovedanega pasu N-tipa silicijevih nanokristaliničnih filmov (tankih plasti). Vrednosti parametrov usklajevanja so izračunali za N-tip nanokristaliničnih filmov z energijo med 1,7 eV in 2,2 eV.

Ključne besede: silicijevi nanokristali, dopiranje, temna prevodnost, lomni količnik

1 INTRODUCTION

Silicon nanocrystals (Si-NCs) have attracted a great deal of interest due to their several potential applications in photovoltaic, photonic and nanoeletronic devices.[1–4] Indeed, the small size, a few nanometer ranges of Si-NCs, causes different properties with respect to crystalline bulk silicon. The wide application fields of Si-NCs are due to their tunable optoelectronic properties obtained by controlling their size, shape and doping level and due to the fact that Si-NCs show quantum size effects and can be produced with processes compatible with a complementary metal oxide semiconductor (CMOS).[5] Si-NCs are generally formed in an insulating matrix such as silicon nitride,[6–8] silicon oxide,[9–12] silicon carbide[12–15] or hydrogenated silicon.[16–19] The high resistivity of the Si-NCs embedded in insulating matrices limits their applications, thus N- or P-type impurity doping is crucial for the manufacturing of devices based on Si-NCs.[20–23] Controlling both electrical and optical properties of devices based on silicon nanocrystals remains a challenge for the required applications. The photo response of Si-NCs is directly related to the light absorption efficiency and electrical properties of silicon nanocrystals. In fact, light is absorbed in silicon nanocrystals by free carriers that diffuse in the insulating matrix by different conduction mechanisms,[13–15,24] inducing the appearance of both the photoconductivity effect and photovoltaic effect. Thus, tailoring and tuning the conductivity and the refractive index are crucial for photovoltaic and optoelectronic applications. The electro-optic effect, which changes a material's index of refraction via an applied electric field, has been observed in a silicon nanocrystal material as it makes this material a good candidate for nonlinear optic applications.[5,25] For photovoltaic applications, the electrical and optical properties of Si-NCs used as the base material of solar cells, are critical for the photo-carrier generation and transport, strongly affecting the cell efficiency.[9,26] As the relationship expression between the dark conductivity and the refractive index remains important, we try, via this work,

*Corresponding author's e-mail:
hakim.haoues@univ-jijel.dz (Hakim Haoues)

to establish a semi-empirical expression relating these two important parameters in doped Si-NC films.

2 DERIVATION OF AN ANALYTICAL MODEL OF ELECTRICAL CONDUCTIVITY OF DOPED SILICON NANOCRYSTALS

In this section, we derive an analytical model including the dark conductivity as a function of the bandgap energy E_g of silicon nanocrystals. We consider a thin layer of doped nanocrystalline silicon as a set of silicon nanocrystallites of the same size, dc, separated by an insulating matrix with thickness d_{in} (intercrystallite regions) and barrier height energy ψ_B.

The Fermi-Dirac statistical distribution of electrons is given by Equation (1):

$$n = N_C \exp\left(\frac{E_{fn} - E_c}{K_B T}\right) \tag{1}$$

where N_c is the effective density of states in the conduction band (BC), which is expressed by Equation (2):

$$N_C = \frac{2}{h^3}(2\pi m_n K_B T)^{3/2} \tag{2}$$

N_c: in cm^{-3};
E_{fn}: electron quasi Fermi level;
E_c: conduction band level;
K_B: Boltzmann constant in eV/K;
T: temperature in Kelvin;
m_n: effective mass of electron in kg;
h: Planck constant in J s.

The intrinsic density of electrons is given by Equation (3):

$$n_i = N_C \exp\left(\frac{E_{fi} - E_c}{K_B T}\right) \tag{3}$$

E_{fi}: intrinsic Fermi level.

Thus the free carrier density (electrons) can be expressed as a function of the intrinsic density as:

$$n = n_i \exp\left(\frac{E_{fn} - E_{fi}}{K_B T}\right) \tag{4}$$

The dark conductivity of the N-type silicon nanocrystal film is given by Equation (5):

$$\sigma_n = qn\mu_{eff} \tag{5}$$

q: electronic charge in coulomb (C);
n: density of free electrons in cm^{-3};
μ_{eff}: effective mobility of electrons in cm^2/Vs.

By integrating Equation (4) into Equation (5) and knowing that the intrinsic Fermi level lies in the middle of the bandgap, $E_g = 2.\ E_{fi}$ (where Eg is the bandgap energy), we obtain:

$$\sigma_n = qn_i\mu_{eff} \exp\frac{E_{fn}}{K_B T} \exp\frac{-E_g}{2K_B T} \tag{6}$$

The intrinsic density n_i can be expressed by Equation (7):

$$n_i = \sqrt{(N_c N_v)} \cdot \exp\frac{-E_{fi}}{K_B T} \tag{7}$$

N_v: effective density of states in the valence band (VB) expressed as:

$$N_v = \frac{2}{h^3}\left(2\pi m_h K_B T\right)^{3/2} \tag{8}$$

N_v: in cm^{-3};
m_h: effective mass of hole in kg.

By integrating Equation (7) into Equation (6) we obtain:

$$\sigma_n = q\mu_{eff}\sqrt{(N_c N_v)} \exp\left(\frac{E_{fn} - E_{fi}}{K_B T}\right)\exp\frac{-E_g}{2K_B T} \tag{9}$$

The ratio between the free carrier density (electrons) and the intrinsic density deduced from Equation (4) is:

$$\left(\frac{n}{n_i}\right) = \exp\left(\frac{E_{fn} - E_{fi}}{K_B T}\right) \tag{10}$$

Integrating Equation (10) into Equation (9) gives:

$$\sigma_n = q\mu_{eff}\sqrt{(N_c N_v)}\left(\frac{n}{n_i}\right)\exp\frac{-E_g}{2K_B T} \tag{11}$$

Considering $R_n = (n/n_i)$, the ratio between the free carrier density and the intrinsic density, the dark conductivity expression of N-type silicon nanocrystals can be rewritten as:

$$\sigma_n = q\mu_{eff}\sqrt{(N_c N_v)}R_n \exp\frac{-E_g}{2K_B T} \tag{12}$$

For P-type silicon nanocrystal films term R_n is replaced by R_p, given by $R_p = (P/n_i)$, where p represents the free hole density.

The effective carrier mobility μ_{eff} can be calculated using the following expression:[27]

$$\mu_{eff} = \frac{\mu_c}{1 + F\left(\frac{\mu_c d_{in}}{d_c \mu_{in}}\right)\exp\left(\frac{\psi_B}{K_B T}\right)} \tag{13}$$

d_c: average crystallite size in nanometer (nm);
d_{in}: intercrystallite distance in nanometer (nm);
F: factor given by $F = 1 - (d_c/L)$ where L is the total length of the film in nanometer;
μ_{in}: mobility in intercrystalline regions;
ψ_B: barrier height energy of intercrystalline regions;
μ_c: mobility in crystalline regions taken as the mobility in monocrystalline silicon given by Equation (14):[28]

$$\mu_c = \frac{\mu_{max} - \mu_{min}}{1 + \left(\frac{N}{N_{ref}}\right)^{\alpha}} + \mu_{min} \tag{14}$$

N: free carrier density.

The values of μ_{max}, μ_{min}, N_{ref} and α are tabulated in Reference[28].

3 MODEL VALIDATION

Our study is based on the experimental results by W. He et al.[29] concerning films of phosphorus doped silicon nanocrystals embedded in amorphous silicon matrix. These results show the dependence of free carrier density, dark conductivity and free carrier mobility on the silicon nanocrystal size.

First, we examine the validity of Equation (13) to describe the experimental effective carrier mobility values. **Figure 1** depicts the variation in the carrier mobility as a function of free carrier density. We can clearly observe a good agreement between experimental and theoretical results. Thus, Equation (13) describes well the effective carrier mobility in doped silicon nanocrystals. The best adjustment parameters are summarized in **Table 1** including several crystallite sizes taken from Ref.[29] The intercrystallite distance d_{in} values are taken to be around 1 nm.[30] The optimal value of μ_{in} that allows the best superposition between the experimental and theoretical curves is 0.08 cm²/V·s.

Table 1: Adjustment parameters as a function of crystallite size

d_c(nm)	F	ψ_B(eV)
6.76	0.986	0.011
5.59	0.989	0.012
4.67	0.991	0.018
4.31	0.9914	0.027
3.59	0.9929	0.0275

Figure 2 represents the comparison between the experimental and theoretical dark conductivities as a function of bandgap E_g. It is worth noticing that the experimental values from Ref.[29] are given as a function of the Si-NC size. To be able to plot the experimental curve of

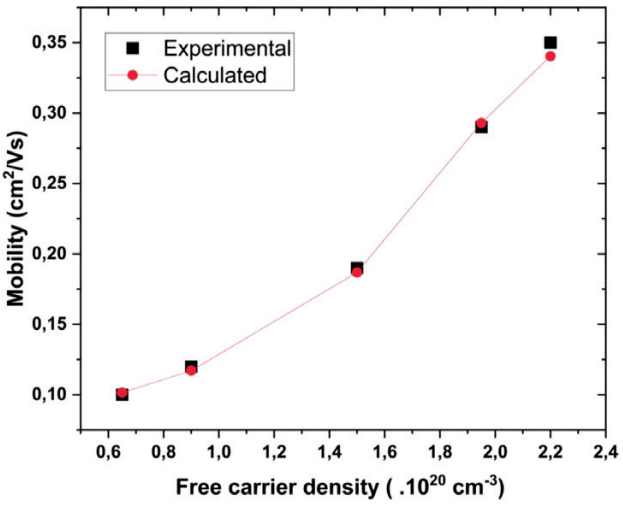

Figure 1: Variation in the calculated and experimental[29] carrier mobility as a function of free carrier density

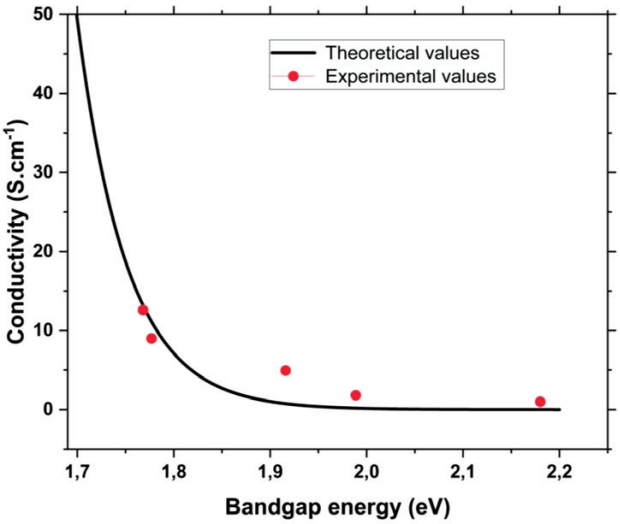

Figure 2: Comparison between the experimental[29] and theoretical dark conductivities as a function of bandgap energy

the conductivity as a function of E_g, we proceed to determine the values of E_g as a function of the silicon nanocrystallite size using the expression below.[31]

$$E_g(d_c) = E_g(\infty) + \frac{3.4382}{d_c} + \frac{1.1483}{(d_c)^2} \qquad (15)$$

$E_g(d_c)$ is the silicon nanocrystallites bandgap as a function of the nanocrystallite size, $E_g(\infty)$ is the bulk bandgap energy of silicon.

E_g is expressed in eV and d_c in nanometers (nm).

The best agreement between the two curves from **Figure 2** is obtained for an average value of $R_n.\mu_{eff}$ equal to 4.2.10¹⁵ cm²/(V·s).

4 RELATIONSHIP BETWEEN DARK CONDUCTIVITY AND REFRACTIVE INDEX

From Equation (12) and the empirical expression giving the refractive index η as a function of E_g, we try to

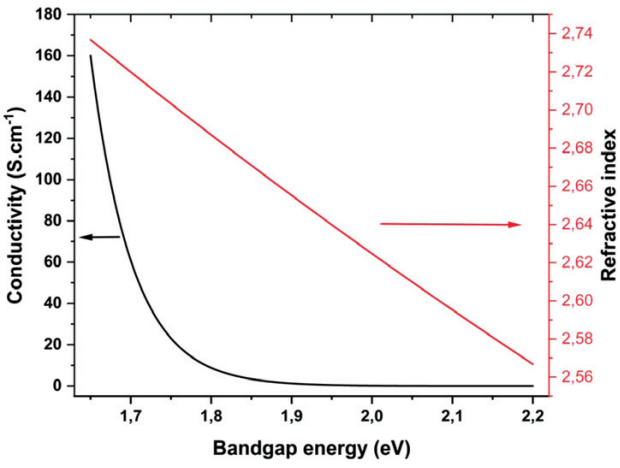

Figure 3: Variation in the dark conductivity and refractive index as a function of bandgap energy

determine the relationship between the electrical conductivity and the refractive index.

Indeed, the refractive index can be determined using Equation (16):[32]

$$\eta^2 - 1 = \frac{A}{(E_g + B)^2} \quad (16)$$

where $A = 25\ E_g + 212$ eV and $B = 0.21\ E_g + 4.25$ eV

Figure 3 represents the variation in the dark conductivity and the refractive index as a function of bandgap E_g. The curve giving the variation in the dark conductivity as a function of the refractive index can therefore be deduced. Indeed, we use the theoretical data from **Figure 2** giving the variation in the dark conductivity as a function of bandgap energy that agrees well with the experimental results from Ref.[29] In **Figure 4**, we superpose the results obtained with our approach, their fit and the experimental results published in Ref.[33] for comparison. We can clearly see that the experimental results agree well with the calculated results. The best fit of our results, giving the dark conductivity as a function of refractive index, can be expressed with the following equation:

$$\sigma + \sigma' = \sigma'' \cdot \exp\frac{\eta - \eta_0}{\tau} \quad (17)$$

where σ is expressed in S·cm^{-1}, $\eta_0 = 2.56$, $\tau = 0.016$, $\sigma' = 8.29.10^{-4}$ S·cm^{-1}, $\sigma'' = 46.8 \times 10^{-4}$ S·cm^{-1}.

The fit parameters are calculated for the bandgap energy values of N-type Si-NC films between 1.7 eV and 2.2 eV.

5 CONCLUSIONS

A correlation method providing a relationship between the dark conductivity and refractive index of N-type silicon nanocrystal films was developed based on experimental data. We first derived an analytical expression giving the dark conductivity as a function of bandgap energy. This expression was combined with an empirical expression relating the refractive index to the bandgap energy and thus a semi-empirical relationship between the dark conductivity and refractive index was established. In order to validate the semi-empirical approach, we compared the results obtained with the proposed approach with the experimental results. A reasonably good agreement was observed for a variation interval in the bandgap energy.

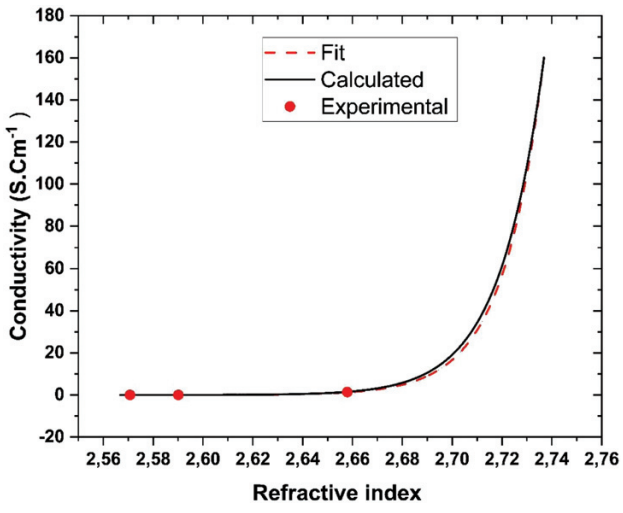

Figure 4: Variation in the dark conductivity as a function of refractive index (experimental data[33])

6 REFERENCES

[1] H. Tan, P. Babal, M. Zeman, A. H. M. Smets, Wide bandgap p-type nanocrystalline silicon oxide as window layer for high performance thin-film silicon multi-junction solar cells, Solar Energy Materials & Solar Cells, 132 (**2015**), 597–60, doi:10.1016/j.solmat.2014.10.020

[2] S. Zhao, X. Liu, X. Pi, D. Yang, Light-emitting diodes based on colloidal silicon quantum dots, J. Semicond., 39 (**2018**) 6, doi:10.1088/1674-4926/39/6/061008

[3] G. Conibeer, M. Green, R. Corkish, Y. Cho, E. Cho, C. Jiang, T. Fangsuwannarak, E. Pink, Y. Huang, T. Puzzer, T. Trupke, B. Richards, A. Shalav, K. Lin, Silicon nanostructures for third generation photovoltaic solar cells, Thin Solid Films, 511–512 (**2006**), 654–662, doi:10.1016/j.tsf.2005.12.119

[4] A. T. Hatzopoulos, I. Pappas, D. H. Tassis, N. Arpatzanis, C. A. Dimitriadisa, Analytical current-voltage model for nanocrystalline silicon thin-film transistors, Appl. Phys. Lett., 89 (**2006**) 19, 193504, doi:10.1063/1.2374851

[5] Z. Bisadi, M. Mancinelli, S. Manna, S. Tondini, M. Bernard, A. Samusenko, M. Ghulinyan, G. Fontana, P. Bettotti, F. Ramiro-Manzano, G. Pucker, L. Pavesi, Silicon nanocrystals for nonlinear optics and secure communications, Phys. Status Solidi A, 212 (**2015**) 12, 2659–2671, doi:10.1002/pssa.201532528

[6] J. López-Vidrier, S. Gutsch, O. Blázquez, J. Valenta, D. Hiller, J. Laube, J. Blanco-Portals, L. López-Conesa, S. Estradé, F. Peiró, B. Garrido, S. Hernández, M. Zacharias, Effect of Si_3N_4-Mediated Inversion Layer on the Electroluminescence Properties of Silicon Nanocrystal Superlattices, Adv. Electron. Mater., 4 (**2018**) 5, 170066, doi:10.1002/aelm.201700666

[7] A. K. Panchal, D. K. Rai, M. Mathew, C. S. Solanki, Silicon quantum dots growth in sinx dielectric: A review, NANO: Brief Reports and Reviews, 4 (**2009**) 5, 265–279 doi:10.1142/S1793292009001770

[8] N. Hafsi, H. Bouridah, M. R. Beghoul, H. Haoues, Photoluminescence from silicon nanocrystals embedded in silicon nitride fabricated by low-pressure chemical vapor deposition followed by high-temperature annealing, J. Appl. Phys., 117 (**2015**) 6, 063105, doi:10.1063/1.4907762

[9] S. H. Hong, Y. S. Kim, W. Lee, Y. H. Kim, J. Y. Song, J. S. Jang, J. H. Park, S. H. Choi, K. J. Kim, Active doping of B in silicon nanostructures and development of a Si quantum dot solar cell, Nanotechnology, 22 (**2011**) 42, 425203, doi:10.1088/0957-4484/22/42/425203

[10] X. J. Hao, E-C. Cho, C. Flynn, Y. S. Shen, G. Conibeer, M. A. Green, Effects of boron doping on the structural and optical properties of silicon nanocrystals in a silicon dioxide matrix, Nanotechnology, 19 (**2008**) 42, 424019, doi:10.1088/0957-4484/19/42/424019

[11] T. Zhang, B. Simonds, K. Nomoto, B. P. Veettil, Z. Lin, I. P. Wurfl, G. Conibeer, Pulsed KrF excimer laser dopant activation in nanocrystal silicon in a silicon dioxide matrix, Appl. Phys. Lett., 108 (**2016**), 083103, doi:10.1063/1.4942466

[12] D. Song, E. C. Cho, G. Conibeer, C. Flynn, Y. Huang, M. A. Green, Structural, electrical and photovoltaic characterization of Si

nanocrystals embedded in a SiC matrix and Si nanocrystals/c-Si heterojunction devices, Solar Energy Materials & Solar Cells, 92 (**2008**) 4, 474–481, doi:10.1016/j.solmat.2007.11.002

[13] A. Kole, P. Chaudhuri, Growth of silicon quantum dots by oxidation of the silicon nanocrystals embedded within silicon carbide matrix, AIP Advances, 4 (**2014**), 107106, doi:10.1063/1.4897378

[14] Z. Xia, S. Huang, Structural and photoluminescence properties of silicon nanocrystals embedded in SiC matrix prepared by magnetron sputtering, Solid State Communications, 150 (**2010**) 19–20, 914–918, doi:10.1016/j.ssc.2010.02.032

[15] J. López-Vidrier, P. Löper, M. Schnabel, S. Hernández, M. Canino, C. Summonte, S. Janz, B. Garrido, Silicon nanocrystals embedded in silicon carbide as a wide-band gap photovoltaic material, Solar Energy Materials & Solar Cells, 144 (**2016**), 551–558, doi:10.1016/j.solmat.2015.10.006

[16] W. Wensheng, W. Tianmina, Z. Chunxi, L. Guohua, H. Hexiang, D. Kun, Preferred growth of nanocrystalline silicon in boron-doped nc-Si:H Films, Vacuum, 74 (**2004**) 1, 69–75, doi:10.1016/j.vacuum.2003.11.008

[17] H. Chen, W. Z. Shen, W. S. Wei, Photoluminescence and Raman Studies on Boron-Doped Nanocrystalline Si:H Thin Films, Solid State Phenomena, 121–123 (**2007**), 933–938, doi:10.4028/www.scientific.net/SSP.121-123.933

[18] H. Chen, M. H. Gullanar, W. Z. Shena, Effects of high hydrogen dilution on the optical and electrical properties in B-doped nc-Si:H thin films, Journal of Crystal Growth, 260 (**2004**) 1–2, 91–101, doi:10.1016/j.jcrysgro.2003.08.048

[19] W. He, A. Zakar, T. Roger, I. V. Yurkevich, A. Kaplan, Determination of recombination coefficients for nanocrystalline silicon embedded in hydrogenated amorphous silicon, Optics Letters, 40 (**2015**) 16, 3889–3892, doi:10.1364/OL.40.003889

[20] M. Xie, D. Li, L. Chen, F. Wang, X. Zhu, D. Yang, The location and doping effect of boron in Si nanocrystals embedded silicon oxide film, Appl. Phys. Lett., 102 (**2013**), 123108, doi:10.1063/1.4798834

[21] D. Ma, J. Liu, W. Zhang, Investigation of Silicon Quantum Dots Embedded in Boron-Doped Silicon Oxide Thin Films Prepared by PECVD Applying Ar Dilution, Phys. Status Solidi A, 215 (**2018**) 2, 1700682, doi:10.1002/pssa.201700682

[22] X. Pi, Doping Silicon Nanocrystals with Boron and Phosphorus, J. Nanomater., 2012 (**2012**), 912903, doi:10.1155/2012/912903

[23] S. H. Hong, Y. S. Kim, W. Lee, Y. H. Kim, J. Y. Song, J. S. Jang, J. H. Park, S. H. Choi, K. J. Kim, Active doping of B in silicon nanostructures and development of a Si quantum dot solar cell, Nanotechnology, 22 (**2011**) 42, 425203, doi:10.1088/0957-4484/22/42/425203

[24] D. J. Norris, A. L. Efros, S. C. Erwin, Doped Nanocrystals, Science, 319 (**2008**) 5871, 1776, doi:10.1126/science.1143802

[25] G. Vijaya Prakash, M. Cazzanelli, Z. Gaburro, L. Pavesi, F. Iacona, G. Franzò, F. Priolo, Nonlinear optical properties of silicon nanocrystals grown by plasma-enhanced chemical vapor deposition, J. Appl. Phys., 91 (**2002**), 4607, doi:10.1063/1.1456241

[26] D. Di, H. Xu, I. Perez-Wurfl, M. A. Green, G. Conibee, Improved nanocrystal formation, quantum confinement and carrier transport properties of doped Si quantum dot superlattices for third generation photovoltaics, Prog. Photovolt.: Res. Appl., 21 (**2011**) 4, 269–277, doi:10.1002/pip.1230

[27] N. Gupta, B. P. Tyagi, An Analytical Model of the Influence of Grain Size on the Mobility and Transfer Characteristics of Polysilicon Thin-Film Transistors (TFTs), Physica Scripta, 7 (**2005**) 2, 225–228, doi:10.1238/Physica.Regular.071a00225

[28] D. M. Caughey, R. Thomas, Carrier mobilities in silicon empirically related to doping and field, Proceedings of the IEEE, 55 (**1967**) 12, 2192–2193, doi:10.1109/PROC.1967.6123

[29] W. He, Z. Li, C. Wen, H. Liu, W. Shen, Size dependence of phosphorus doping in silicon nanocrystals, Nanotechnology, 27 (**2016**) 42, 425710, doi:10.1088/0957-4484/27/42/425710

[30] C. W. Jiang, M. A. Green, Silicon quantum dot superlattices: Modeling of energy bands, densities of states, and mobilities for silicon tandem solar cell applications, J. Appl. Phys., 99 (**2006**), 114902, doi:10.1063/1.2203394

[31] X. Peng, S. Ganti, P. Sharma, A. Alizadeh, S. Nayak, S. Kumar, Novel Scaling Laws for Band Gaps of Quantum Dots, J. Comput. Theor. Nanosci., 2 (**2005**) 3, doi:10.1166/jctn.2005.202

[32] D. K. Ghosh, L. K. Samanta, G. C. Bhar, A simple model for evaluation of refractive
indices of some binary and ternary mixed crystals, Infrared Phys., 24 (**1984**) 1, 43–47, doi:10.1016/0020-0891(84)90046-0

[33] L. Mazzarella, A. B. Morales-Vilches, M. Hendrichs, S. Kirner, L. Korte, R. Schlatmann, B. Stannowski, Nanocrystalline n-Type Silicon Oxide Front Contacts for Silicon Heterojunction Solar Cells: Photocurrent Enhancement on Planar and Textured Substrates, IEEE Journal of Photovoltaics, 8 (**2018**), 70–78, doi:10.1109/JPHOTOV.2017.2770164